Cerebral Cortex August 2012;22:1923–1934
doi:10.1093/cercor/bhr265
Advance Access publication October 6, 2011

Laterality of Temporoparietal Causal Connectivity during the Prestimulus Period Correlates with Phonological Decoding Task Performance in Dyslexic and Typical Readers

Richard E. Frye[1], Jacqueline Liederman[2], Janet McGraw Fisher[3] and Meng-Hung Wu[4]

[1]Division of Child Neurology, Arkansas Children's Hospital, Little Rock, AR 72202, USA, [2]Department of Psychology, Boston University, Boston, MA 02215, USA, [3]Department of Psychology, State University of New York Westchester County, Valhalla, NY 10595, USA and [4]Department of Computer Science, South Texas College, McAllen, TX 78501, USA

Address correspondence to Richard E. Frye, Division of Child Neurology, Arkansas Children's Hospital, 1 Children's Way, Little Rock, AR 72202 USA. Email: REFrye@uams.edu.

We examined how effective connectivity into and out of the left and right temporoparietal areas (TPAs) to/from other key cortical areas affected phonological decoding in 7 dyslexic readers (DRs) and 10 typical readers (TRs) who were young adults. Granger causality was used to compute the effective connectivity of the preparatory network 500 ms prior to presentation of nonwords that required phonological decoding. Neuromagnetic activity was analyzed within the low, medium, and high beta and gamma subbands. A mixed-model analysis determined whether connectivity to or from the left and right TPAs differed across connectivity direction (in vs. out), brain areas (right and left inferior frontal and ventral occipital–temporal and the contralateral TPA), reading group (DR vs. TR), and/or task performance. Within the low beta subband, better performance was associated with increased influence of the left TPA on other brain areas across both reading groups and poorer performance was associated with increased influence of the right TPA on other brain areas for DRs only. DRs were also found to have an increase in high gamma connectivity between the left TPA and other brain areas. This study suggests that hierarchal network structure rather than connectivity per se is important in determining phonological decoding performance.

Keywords: dyslexia, effective connectivity, Granger causality, magnetoencephalography, reading

Introduction

Developmental dyslexia is the most common learning disorder worldwide, affecting both children and adults with a prevalence as high as 17.5% (Shaywitz 1998). Dyslexia is a lifelong disorder with a wide variability in prognosis regardless of the quality of remediation therapy. Some studies have suggested that 2 subsets of dyslexic readers (DRs) can be differentiated based on the reading skills that they eventually develop as young adults: one subset is believed to develop adequate phonological word decoding skills as young adults and the other subset is believed to continue to manifest poor phonological word decoding skills into adulthood (Shaywitz et al. 2003; Miller-Shaul 2005; Svensson and Jacobson 2006). In contrast, other studies suggest that DRs are probably best represented on a continuum of severity with multiple genetic and environmental risk factors interacting to result in the phenotype known as dyslexia (Pennington and Lefly 2001; Snowling 2008). Recently, we demonstrated that brain morphology (Frye, Liederman, Malmberg, et al. 2010), white matter connectivity (Frye, Hasan, et al. 2008; Frye, Liederman, Hasan, et al. 2010), and effective connectivity (Frye, Wu, et al. 2010) were related to reading-related skills on a continuum in young adults with a history of dyslexia, thereby supporting the latter notion.

Three regions of the brain often manifest atypical activation in DRs as compared with typical readers (TRs). These areas include the inferior frontal areas (IFAs), the temporoparietal areas (TPAs), and the ventral occipital–temporal areas (VOTAs; Pugh, Mencl, Jenner, et al. 2000). This study will focus on the TPAs and their connection to these other 2 brain areas as well as to each other. The TPAs are the most consistently reported areas of the brain that manifest atypical functional activation in DRs. Relative underactivation of the left TPA and overactivation of the right TPA has been reported in DRs during early childhood (Simos, Fletcher, Foorman, et al. 2002), later childhood (Temple et al. 2003), adolescence (Simos, Fletcher, Bergman, et al. 2002), and adulthood (Shaywitz et al. 2003). Several studies have indicated that atypical TPA functional activation can change with remediation. However, the exact changes in right and left TPA functional activation have been inconsistent across studies. Some studies report an increase in left TPA activation in children with dyslexia who respond to intensive intervention (Simos et al. 2007). However, other studies report that functional activation of both the right and the left TPAs increase following interventions in children with dyslexia (Temple et al. 2003). Furthermore, other data suggest that atypical right TPA functional overactivation may persist into adulthood for DRs who develop adequate phonological decoding accuracy but continue to have slow decoding skills and remain nonfluent readers (Shaywitz et al. 2003). Thus, whether persistence of atypical right TPA activity is compensatory or disadvantageous remains under question (Shaywitz et al., 2003, 2006).

Rather than comparing functional activation between DRs and TRs, some have compared functional connectivity. Two early studies demonstrated poorer connectivity between the left VOTA and TPA in DRs as compared with TRs (Horwitz et al. 1998; Pugh, Mencl, Shaywitz, et al. 2000). Newer connectivity techniques allow the study of effective connectivity. Using such newer techniques it is possible to determine the influence of different cortical areas on each other, not just whether cortical areas are connected to one another. Two of these techniques, structural equation modeling and dynamic causal modeling, are model-based effective connectivity techniques. These techniques require the experimenter to specify a particular set of causal connections between brain areas and then estimate free parameters for these models. These models restrict the number of possible causal connections. As

a consequence, when these techniques have been applied to studies on reading, they have only evaluated one direction of coupling (e.g., feedforward; Levy et al. 2009) or analyzed only the left hemisphere (Cao et al. 2008; Quaglino et al. 2008; Bitan et al. 2009).

In contrast to these "model-driven" techniques for measuring effective connectivity, Granger causality (GC) is a "data-driven" technique that empirically calculates the direction and strength of connectivity with minimal assumptions about the structure of the neural network (Frye, Wu, et al. 2010; Frye and Wu forthcoming; Sakkalis forthcoming; Wu et al. forthcoming). GC is based on the assumption that causes precede effects. To determine the temporal relationship between neurophysiological signals, the GC technique uses autoregressive (AR) models to analyze the temporal relation within and between signals. Essentially, if a particular neurophysiological signal can predicted another neurophysiological signal better than that signal can predict itself, it is considered to be driving the signal.

An AR process can be defined for a time series $A = [a(t): 1 \ldots T]$ and is assumed to have a periodic component so that at any time t it can be predicted by the values of the previous signal. Equation (1) defines signal $a(t)$ which is dependent on the past 3 values at times $t-1$, $t-2$, and $t-3$. The influence of the signal at times $t-1$, $t-2$, and $t-3$ on the current time is given by the coefficients c_1, c_2, and c_3, respectively. Since real signals are not completely deterministic, we must consider that the predicted value of signal $a(t)$ is associated with some error $e_{a|a}(t)$. This error represents the portion of the signal $a(t)$ at time t which is not accounted for by the given previous values of $a(t-1)$, $a(t-2)$, and $a(t-3)$:

$$a(t) = c_{a,1} * a(t-1) + c_{a,2} * a(t-2) + c_{a,3} * a(t-3) + e_{a|a}(t). \quad (1)$$

The number of previous time points considered is known as the order of the model. A generalization of equation (1) for any order P is given by equation (2) where error $e_{a|a}(t)$ represents the portion of the signal $a(t)$ at time t that is not accounted for given the previous values of $a(t-1) \ldots a(t-P)$:

$$a(t) = \sum_{j=1}^{p} c_{a,j} * a(t-j) + e_{a|a}(t). \quad (2)$$

A periodic signal can also be predicted by another periodic signal rather than itself. The case where the time series $B = [b(t): 1 \ldots T]$ predicts the time series A is given in equation (3) where the model order is P and $e_{a|b}(t)$ represents the error in predicting $a(t)$ given the previous time point of $b(t-1) \ldots b(t-P)$:

$$a(t) = \sum_{j=1}^{p} c_{b,j} * b(t-j) + e_{a|b}(t). \quad (3)$$

The signal $a(t)$ can also be predicted by its own past activity as well as activity of another signal. In order to formulate such a model, we combine equations (2) and (3) to produce equation (4). Equation (4) demonstrates that signal $a(t)$ at time t is being predicted by the previous activity of both $a(t-1) \ldots a(t-P)$ and $b(t-1) \ldots b(t-P)$. $e_{a|ab}(t)$ represents the error in predicting $a(t)$ given the previous time point of $a(t-1) \ldots a(t-P)$ and $b(t-1) \ldots b(t-P)$:

$$a(t) = \sum_{j=1}^{p} c_{a,j} * a(t-j) + \sum_{k=1}^{p} c_{b,j} * b(t-k) + e_{a|ab}(t). \quad (4)$$

GC measures the influence of one signal on another. This measure is based on the relative change in the model error when time series are added to improve the prediction of the dependent signal (Granger 1969). For example, we can measure the error accounted for by adding the time series B to equation (4) by comparing the error terms of equations (2) and (4). The traditional GC measure is given by equation (5) (Ding et al. 2006; Seth and Edelman 2007). Essentially GC is the ratio of the variance of the model before and after the addition of the new time series:

$$F_{y \to x} = \ln \frac{\mathrm{Var}(e_{a|a})}{\mathrm{Var}(e_{a|ab})}. \quad (5)$$

Although Granger originally described using least-square linear regression for solving AR models (Granger 1969), over the last 2 decades many researchers, particularly those in the signal analysis field, have adopted the Levinson, Wiggins, Robinson algorithm, a maximum entropy method, to solve the system of AR equations associated the GC (Ding et al. 2000, 2006). Recently, we demonstrated that a version of GC analysis that uses least-squares linear regression known as Dynamic Autoregressive Neuromagnetic Causal Imaging (DANCI) has significant advantages over a method that uses the Levinson, Wiggins, Robinson algorithm and that DANCI provides a fast, accurate, unbiased, and robust estimation of GC for up to 50 completely interconnected neurophysiological signals (Frye and Wu forthcoming). In addition, although GC is traditionally a time domain method, the concept has been adapted to the frequency domain (Geweke 1984; Hosoya 2001) for which several alternate causality measures, such as the directed transfer function (Kaminski and Blinowska 1991) and partial directed coherence (Sameshima and Baccala 1999), have been developed. Recently, we demonstrated that GC provides a more accurate estimation of effective connectivity than these other frequency domain measures (Wu et al. forthcoming).

We recently used DANCI to analyze neuromagnetic causal connectivity during the prestimulus period while DR and TR participants were preparing to phonologically decode a visually presented nonword (Frye, Wu, et al. 2010). We compared causal connectivity between the IFA and brain areas known to be essential for reading (left and right IFAs, TPAs, and VOTAs) in the low, medium, and high beta and the low, medium, and high gamma frequency subbands. We found that greater top-down connectivity from the left IFA to other cortical regions in the low beta subband was correlated with better phonological task performance in DRs but not TRs, suggesting that left IFA top-down activity may be acting in a compensatory manner to facilitate phonological decoding in DRs.

In contrast, TRs did not demonstrate significant top-down activity from either the left or the right IFA to other key brain regions. We hypothesized that this was due to the fact that the reading network in TRs did not require top-down activation from the frontal areas since the reading network in TRs is believed to automatically engage when phonological word decoding is necessary. In fact, this automaticity is a key attribute that is deficient in DRs (Yap and van der Leij 1994; Brambati et al.

2006; Shaywitz and Shaywitz 2008). This reasoning led us to suggest that in DRs, the atypically strong functional connectivity from the left IFA to other key brain regions for reading may serve them as a compensatory mechanism.

Using GC, our previous study helped clarify why functional overactivation of the left IFA is inconsistently reported in DRs. First, the functional activation of the IFA in DRs probably depends on how well the DR has compensated for their disability, making the results of functional brain imaging studies sensitive to the characteristics of the individuals which make up the group of DRs selected for the study. Second, the influence of the IFA on other brain areas probably depends on IFA causal connectivity, not just functional activation. We believe that the inconsistency across studies in the functional activation of the left and right TPAs in DRs is due to the same factors that we argued affect the inconsistency of IFA activation (Frye, Wu, et al. 2010). These factors are variations in participant performance and differences in causal connectivity between the TPA and other key brain areas involved in reading.

The premise of this study is: 1) in general, the left TPA is the dominant control hub for the preparatory phonological decoding network and 2) in DRs, the extent to which this control is shared with the right TPA is related to deficiencies in phonological decoding performance. Our first set of hypotheses is centered on the causal connectivity measured during beta frequency activation. Beta band activity has been linked to long-range synchronization of the frontal, parietal, temporal, and occipital areas (Gross et al. 2004, 2006) and multimodal integration between cortical lobes (von Stein et al. 1999). Therefore, it is hypothesized that activity within the beta frequency band will be related to large-scale communication between the cortical areas hypothesized above. Specifically, we hypothesize that, in the beta frequency band, 1) for both TRs and DRs, the extent to which the left TPA provides control over the other key cortical regions for reading will be proportional to performance on the nonword phonological decoding task and 2) in only DRs, the extent to which the right TPA also provides control of the key reading areas in the brain will be inversely proportional to performance on the nonword phonological decoding task. We used GC to examine the influence from the right or left TPA to other brain areas relative to the influence from other brain areas to the right or left TPA. Greater relative influence of the right or left TPA on other brain regions will be interpreted as a measure of control over those regions.

In contrast to beta band activity, we hypothesize that increased levels of gamma-band interconnectivity between the TPA and other brain regions will be associated with decreased performance during phonological decoding. In our prior study (Frye, Wu, et al. 2010), stronger symmetric gamma-band connectivity between the IFA and other key brain areas involved in reading during the prestimulus period was found to be related to poorer performance on the visual phonological decoding task. Transient desynchronization of gamma activity has been documented during reading in TRs (Lachaux et al. 2008). Therefore, we interpreted our results as indicating that high preparatory gamma-band connectivity may have reduced the ability of the network to decouple during the performance of the actual task and assume an asymmetric activation pattern. We now are testing whether high levels of gamma in the TPAs are also associated with poorer phonological decoding.

Materials and Methods

Participants

We examined 10 TRs and 7 DRs who were native English speakers between the ages of 18 and 45 years, with normal or corrected vision, normal hearing, and no history of severe psychiatric or neurological illnesses or attention defects. DRs reported a childhood diagnosis of phonological dyslexia and were either referred from the Office of Disability Services at Boston University or recruited from Curry College in Milton, Massachusetts.

Reading performance composite was calculated by averaging the percentile ranks of reading rate and comprehension of the Nelson–Denny Reading Test. DRs scored below and TRs scored above the 25th percentile. All participants scored greater than or equal to 80 on the Wechsler Adult Intelligence Scale as estimated from vocabulary and block design subtests (Wechsler 1997) and subtest scores were equivalent for DRs and TRs (Table 1). Right handedness was confirmed by a score greater than 50 on the Edinburgh Handedness Inventory (Dragovic 2004). Written informed consent was obtained in accordance with our Institutional Review Board regulations. Participants underwent a magnetoencephalography (MEG) and magnetic resonance imaging (MRI) scan as described below and received $20 per hour.

Participants completed additional tasks that measured their phonological skills (McGraw Fisher et al. forthcoming). Two tasks that complemented the nonword rhyme task performed in the scanner are discussed (McGraw Fisher et al. forthcoming). In the first task, called the final consonant discrimination task, participants completed an auditory discrimination task that required speech sound segmentation. One-syllable nonword synthetic stimuli with a consonant-vowel-consonant (CVC) structure were synthesized such that the vowel segments were not the same. This allowed trials with a rhyming stimuli pair in which the final consonant was the same and trials with nonrhyming stimuli pair in which the final consonants were not the same. Participants listened to 48 pairs of CVC nonwords separated by a 250 ms interstimulus interval and decided if the final consonant sounds were the same or different. As seen in Table 1, accuracy on the final consonant task was lower for DRs as compared with TRs (t_{16} = 3.30, $P < 0.01$). Similarly latencies were longer for DRs as compared with TRs (t_{16} = 2.35, $P < 0.05$). In the second task, called the nonword naming task, participants were required to pronounce 40 two-syllable nonwords aloud. This task explicitly measured phonological decoding ability as a nonphonological strategy could not be used to successfully complete this task. Accuracy on the nonword naming task was lower for the DRs as compared with TRs (t_{16} = 2.18, $P < 0.05$). Reaction time for the nonword naming task was higher for the DRs as compared with the TRs but the difference did not reach statistical significance.

Nonword Rhyme Task

A scanner task was developed to equate task difficulty across the 2 groups of readers due to their different levels of reading skills (McGraw Fisher et al. forthcoming). In order to do this, we developed a task with 3 levels of difficulty (Fig. 1). For all levels of difficulty, the participant was required to indicate if any of the target nonword(s) rhymed with the test nonword. A keypad press with the right index or middle finger

Table 1
Participant characteristics (mean (standard error))

Characteristic	TRs	DRs
Age	21.9 (1.1)	24.6 (2.3)
Male:female	5:5	3:4
Handedness	77.8 (5.4)	87.1 (4.0)
Nelson–Denny rate	38% (7%)	6% (2%)
Nelson–Denny comprehension	66% (10%)	13% (5%)
Nelson–Denny average	53% (7%)	11% (3%)
Vocabulary subtest	12.9 (1.0)	13.1 (1.3)
Block design subtest	12.6 (0.6)	11.3 (0.7)
Final consonant test—accuracy	84% (2%)	74% (2%)
Final consonant test—reaction time	1862 (123) ms	2659 (314) ms
Nonword naming—accuracy	93% (1%)	79% (6%)
Nonword naming—reaction time	755 (64) ms	1411 (450) ms

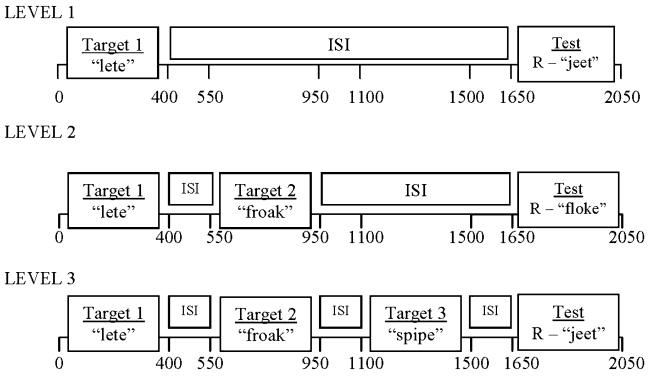

Figure 1. Diagrammatic representation of the nonword rhyme task, including the details of each of the 3 levels.

indicated that the words did or did not rhyme, respectively. All nonwords were presented for 400 ms each, the total time from trial onset to the onset of the test nonword remained constant at 1650 ms and the intertrial interval was 2000 ms. Depending on the level of difficulty, 1, 2, or 3 target nonwords were presented sequentially before the test nonword. By eliminating the most difficult level of the task for the DRs, we were able to achieve overall equivalent performance across these 2 reading groups since DRs performed at chance at the most difficulty level (McGraw Fisher et al. forthcoming). Thus, TRs completed 6 blocks: 4 with 1 target item (level 1), 1 with 2 target items (level 2), and 1 with 3 target items (level 3). DRs completed 5 blocks: 4 with 1 target item (level 1) and 1 with 2 target items (level 2). Each testing block consisted of 60 randomly presented novel trials. Visual stimuli were projected by a Panasonic DLP projector (Model No. PT-D7500U) through an aperture in the chamber onto the back of a nonmagnetic screen located 1.5 m in front of the participant.

Letter strings were constructed to look orthographically similar, even when they did not rhyme, in order to eliminate the use of a visual strategy. For example, the nonwords in the pair "plord/glurd" are similar in length, in the number and position of consonants (C) and vowels (V), but do not rhyme. A visual scan of the overall shape of the nonwords would falsely suggest that they rhyme, since they both end in "rd." Additionally, nonwords that did rhyme did not have the same endings. For example, the nonword pair "leat" and "jete" have different endings but rhyme. Therefore, a correct response could not be based solely on a visual strategy and individuals were required to phonologically decode the nonword in order to correctly complete the task. The task used in the MEG scanner was developed on a larger group of 31 TRs and 26 DRs in order to validate the performance of this task in the 2 groups (McGraw Fisher et al. forthcoming).

Performance Measurements

A signal detection paradigm was used to obtain a measurement of performance without response bias. Rhyme trials were considered signal + noise trials, while nonrhyme trials were considered noise trials. Sensitivity (d-prime) was calculated from the hit and false alarm rates assuming an equal variance model (i.e., z(Hit Rate) – z(False Alarm Rate)).

Magnetic Resonance Imaging

After the MEG session, a high-resolution, 3D, T_1-weighted structural MRI of the brain was acquired. Using FreeSurfer software, the MRI images were segmented and the cortical surface was reconstructed (Dale et al. 1999; Fischl et al. 1999). These images were used to ensure that the MEG sensors selected were located above the true regions of interest.

MEG Acquisition

Participant Preparation

Four head position indicator coils were placed on both sides of the forehead and behind the ears. These coils were used to determine the relative position of the head while in the scanner. The coils' positions were measured using a low-intensity magnetic field generated by each coil at the start of each run. The positions of the coils, the nasion, and auricular points and about 70 points on the scalp were recorded with a Polhemus Fastrack (Colchester, VT) 3D digitizer (Hämäläinen et al. 1993). Electrooculography (EOG) electrodes were placed at each temple and above and below the left eye, with the ground on the left lower cheek. Vertical and horizontal EOG was recorded to detect blinks and large eye movements.

MEG Recording

MEG recordings were performed at the Massachusetts General Hospital Athinoula A. Martinos Center for Biomedical Imaging using a whole-head VectorView system (Elekta Neuromag Oy, Finland) inside a high-performance magnetically shielded room (Imedco AG, Switzerland) (Cohen et al. 2002). The device has 306 SQUID (superconducting quantum interference device) sensors arranged in 102 locations within a helmet-shaped array. Each location contained longitudinal and latitudinal planar gradiometers and a magnetometer. Signals were filtered at 0.1–172 Hz and sampled at 601 Hz.

MEG Postprocessing

Blinking and other artifacts were excluded by removing epochs with EOG amplitudes exceeding 150 μV or gradiometer signals exceeding 3000 fT/cm. Typically, 1 or 2 MEG channels were excluded for each participant due to artifacts. To examine the preparatory state activity, the neural activity was extracted from 500 to 0 ms before the onset of the first nonword stimulus on each trial. Approximately 300 trials were extracted for each participant. To reduce the number of channels, the signal amplitude at each location was derived from the longitudinal and latitudinal planar gradiometers as given in equation (6).

$$\text{Signal Amplitude} = \sqrt{\text{longitudinal amplitude}^2 + \text{latitudinal amplitude}^2}. \quad (6)$$

Since activity within the beta and gamma frequency subbands have been linked to phonological and orthographic processes required for reading in MEG, electroencephalogram (EEG), and intracranial studies (Duncan-Milne et al. 2003; Mainy et al. 2008; Matsumoto and Iidaka 2008; Spironelli et al. 2008; Cornelissen et al. 2009; Trebuchon-Da Fonseca et al. 2009; Penolazzi et al. 2010), we examined signals within the low (12–14 Hz), medium (15–19 Hz), and high (20–29 Hz) beta and low (30–59 Hz), medium (60–89 Hz), and high (90–12 0Hz) gamma subbands. Signals were filtered using low-order bidirectional Butterworth filters to prevent frequency and phase distortion and distortion of the causal structure of the data (Florin et al. 2009). The signal was down sampled by a factor of 2 before analysis.

Region of Interest Selection

Data was selected from 24 sensor locations overlying the right and left IFA, TPA, and VOTA. A viewer depicting the exact position of the selected sensors over the 3D model for each participant was used to ensure that the position of the sensors corresponded to the regions of interest for each participant. The average Talairach coordinates of the cortex underlying the center of the groups of sensors for each region of interest are as follows: left IFA –54.2, 22.4, 1.71; left TPA –62.5, –51.1, 30.4; left VOTA –42.8, –62.4, –13.2; right IFA 57.7, 26.7, 7.1; right TPA 58.0, –54.4, 35.8; right VOTA 39.2, –55.1, –14.4.

GC Analysis

To maintain stationarity, a brief "snapshot" of the signal was extracted using the short-window approach (Ding et al. 2000). A 20 point window was incrementally moved across the 500 ms data epoch. The epoch length was 150 data points after downsampling, which fit 131 20 point windows and 131 observations per trial. Given that about 300 data trials were recorded from each participant, approximately 39 300 (i.e., 300 × 131) observations were produced for each participant. The signal was normalized with respect to both amplitude and variation for each individual and ensemble by detrending each trial, normalizing by the trial mean and standard deviation, and then normalizing by the ensemble mean and standard deviation in a point-by-point manner (Ding et al. 2000; Frye, Wu, et al. 2010).

A system of AR models was constructed to represent the mutual influence of S sensors on one another. The MEG signal from a set of sensors [1 ... S], where $S = 24$, with time points [1 ... T], where $T = 20$ (as described above), is given in time series $A = [a_s(t)$: $s = 1 \ldots S$, $t = 1 \ldots T]$. A system of AR models of order P (eq. 7) was used to model the time series. The model order determines the number of coefficients that are used to model each sensor–sensor interaction:

$$\begin{aligned}
a_1(t) &= \sum_{j=1}^{p} c_{1,1,j}\, a_1(t-j) + \sum_{j=1}^{p} c_{1,2,j}\, a_2(t-j) + \ldots \\
&\quad + \sum_{j=1}^{p} c_{1,S,j}\, a_S(t-j) + e_{1|1\ldots S}(t) \\
a_2(t) &= \sum_{j=1}^{p} c_{2,1,j}\, a_1(t-j) + \sum_{j=1}^{p} c_{2,2,j}\, a_2(t-j) + \ldots \\
&\quad + \sum_{j=1}^{p} c_{2,S,j}\, a_S(t-j) + e_{2|1\ldots S}(t) \\
&\ldots \\
&\ldots \\
a_S(t) &= \sum_{j=1}^{p} c_{S,1,j}\, a_1(t-j) + \sum_{j=1}^{p} c_{S,2,j}\, a_2(t-j) + \ldots \\
&\quad + \sum_{j=1}^{p} c_{S,S,j}\, a_S(t-j) + e_{S|1\ldots S}(t). \qquad (7)
\end{aligned}$$

In equation (7), each single equation represents a signal $a_s(t)$ at time t that is predicted by previous values of itself and all other signals. For example, coefficients $c_{1,1,j}$ ($j = 1 \ldots P$) quantitatively describe the influence of the activity of $a_1(t)$ on itself, coefficients $c_{1,2,j}$ ($j = 1 \ldots P$) quantitatively describe the influence of the activity of $a_2(t)$ on $a_1(t)$, and coefficients $c_{1,s,j}$ ($j = 1 \ldots P$) quantitatively describe the influence of signal $a_s(t)$ on $a_1(t)$, etc. Likewise, coefficients $c_{s,1,j}$ ($j = 1 \ldots P$) describe the quantitative influence of signal $a_1(t)$ on signal $a_s(t)$.

In order to solve this system of equations using least-squares linear regression, we define matrix X^o for one data observation o as equation (8). The design matrix given in equation (9) is defined for all observations from equation (8). The dependent matrix defined in equation (10) is then defined from a series of O observations for each signal s. The coefficients for the above set of equations can then be solved for each signal s using the X and Ys (eq. 11). The coefficients derived with (eq. 11) are the same coefficients outlined in equation (7). For each signal s, equation (11) derives a coefficient matrix with coefficients $[c_{s,1,1} \ldots c_{s,1,P} \ldots c_{s,S,1} \ldots c_{s,S,P}]$. Using the coefficients, the error of the AR for each source can be calculated using equation (12). The variance of the model error, also known as the mean squared error (mse) for signal s is shown in equation (13):

$$X^{\circ} = \left[a_1^{\circ}(t-1) \ldots a_1^{\circ}(t-P)\, a_2^{\circ}(t-1) \ldots a_2^{\circ}(t-P) \ldots a_S^{\circ}(t-1) \ldots a_S^{\circ}(t-P)\right], \quad (8)$$

$$X = \left[X^1 \ldots X^O\right]', \quad (9)$$

$$Y_s = \left[a_s^1(t) \ldots a_s^O(t)\right], \quad (10)$$

$$c_s = (X'X)^{-1}(X'Y_s), \quad (11)$$

$$e_{s|1\ldots S} = Xc_s - Y_s, \quad (12)$$

$$mse_{s|1\ldots S} = \frac{\sum_{i=1}^{O} e_{s|1\ldots S}^2}{O}. \quad (13)$$

We can apply the same calculation to the system of AR models presented in equation (7) to help derive measures of GC. The AR models for a signal s in equation (7) already accounts for the influence of all of signals. We can eliminate the signal of interest by reconstructing the matrix X^o leaving out the signal of interest. For example, if we were interested in the influence of signal 2 on any other signal s, we would reformulate X^o as demonstrated in equation (14), recalculate the least-squares linear regression and derive the error vector $e_{s|1,3\ \ldots\ S}$:

$$X^{\circ} = \left[a_1^{\circ}(t-1) \ldots a_1^{\circ}(t-P)\, a_3^{\circ}(t-1) \ldots a_3^{\circ}(t-P) \ldots a_S^{\circ}(t-1) \ldots a_S^{\circ}(t-P)\right]. \quad (14)$$

The GC measure representing the influence of signal 2 on signal s given all of the other signals 1 to S (expect for 2) would be calculated with equation (15):

$$F_{2\to s} = \ln \frac{mse_{s|1,3\ldots S}}{mse_{s|1\ldots S}}. \quad (15)$$

Using the approach above, we constructed a matrix of GC values to represent the influence of each MEG sensor on every other MEG sensor. We then evaluated the significance of each GC value in order to consider only the connections which represented significant connectivity. The same measure of error that is used to calculate GC can also be used in a partial F-test in order to calculate the significance of the GC value. Equation (16) outlines the calculation of this F-distributed value which has P and $O^*T - S^*P - 1$ degrees-of-freedom in the numerator and denominator, respectively. Granger used the same symptom "F" to signify GC, making the notation confusing:

$$F_{P,O*T-S*P-1}^{2\to s} = \frac{\frac{O\cdot(mse_{s|1,3\ldots S} - mse_{s|1\ldots S})}{P}}{\frac{O\cdot mse_{s|1\ldots S}}{O\cdot T - S\cdot P - 1}}. \quad (16)$$

To empirically derive the structure of the network, we use equation (16) to determine the true connections within the network. The F value in equation (16) provides an indication of statistical significant of the GC value. In order to ensure, we only examine the correct network connections, we use a very conservative alpha ($P \leq 10^{-4}$). In order to compare network connectivity across participants, the average GC values between each language area of interest were calculated by averaging the significant GC values between language areas. This whole process was performed for each frequency band separately.

The optimal model order is typically chosen by estimating several AR models with different orders and determining which model order is optimal with respect to 2 standard information criteria, the Akaike information criterion (AIC) and the Bayesian information criterion (BIC). Since there is no specific criterion to guide the choice of model orders to test, we selected orders 8, 12, and 16. A model order of 16 was found to be optimal with respect to the AIC and BIC criteria.

Statistical Analysis

In order to quantitatively analyze GC values, we constructed a linear mixed-model similar used in our recent studies (Frye et al. 2007; Frye, Fisher, et al. 2008; Frye, Hasan, et al. 2008; Frye et al. 2009; Frye, Liederman, Hasan, et al. 2010; Frye, Liederman, Malmberg, et al. 2010; Frye, Wu, et al. 2010). In our previous studies, we investigated the relationship between performance and anatomic connectivity and found that this relation was not necessarily the same for different reading groups (i.e., DRs, TRs). Thus, our previous models contained the fixed effects of both reading groups (TRs vs. DRs) and a covariate for performance with an additional interaction between these effects. In the current study, we examined effective connectivity to/from the TPA. Since there are 2 directions of connectivity for each connection (in vs. out) an additional fixed effect of connectivity direction was included in the models. Since each TPA is connected to 5 other areas (i.e., right and left IFA, right and left VOTA, and the contralateral TPA) an additional fixed effect, which represented brain area, was included in the model. Thus, the final model for this study had fixed effects of area (5 levels), reading group (TRs vs. DRs), and connectivity direction (in vs. out) with a covariate representing performance, which in this case is d-prime (i.e., sensitivity). The "mixed" procedure of SAS 9.1 (SAS Institute Inc., Cary, NC) was used to evaluate the model. The participants' cortical areas and connectivity direction were entered as random effects in the mixed model (Frye, Wu, et al. 2010).

The general mixed model is in the matrix form is given by equation (17), where y is the dependent variable, which in this case is connectivity between 2 cortical regions, X is the design matrix for the fixed effects and covariate, β is a vector containing the parameters of the fixed effects and covariate, Z is the design matrix for the random effects, γ contains the parameters of the random effects, and ε is the variance–covariance matrix of the model error:

$$y = X\beta + Z\gamma + \varepsilon. \quad (17)$$

The key assumption of the mixed model are that both γ and ε have the expected value of 0 (i.e., E(γ) = 0 and E(ε) = 0) and known covariance structure given by the matrixes Var(γ) and Var(ε). The values for each row of the design matrix X are given by equation (18), where c is the constant with value 1, area is the cortical area represented by the 5 dummy variables $area_1 \ldots area_5$ (i.e., for analysis of the left TPA, dummy variables would be set up to represent the other cortical regions that the left TPA is connected to, e.g., $area_1$ = 1 for left IFA and 0 otherwise, $area_2$ = 1 for left VOTA and 0 otherwise, etc.), inout is connectivity direction represented by a dummy variable (i.e., inward = 0, outward = 1), read is reading group as represented by a dummy variable (i.e., dyslexia = 1, typical = 0) and d_p is the centered d-prime value for the particular participant, p:

$$\begin{aligned} x(t, v, h, a_p, v) = & \\ & [c\ area_1\ area_2\ area_3\ area_4\ area_5\ inout\ read\ d_p\ (area_1 * inout) \\ & \ldots (area_5 * inout)(area_1 * read) \ldots (area_5 * read)(area_1 * d_p) \ldots \\ & (area_5 * d_p)(inout * read)(inout * d_p)(read * d_p) \\ & (area_1 * inout * read) \ldots (area_5 * inout * read)(area_1 * inout * d_p) \\ & \ldots (area_5 * inout * d_p)(area_1 * read * d_p) \ldots (area_5 * read * d_p) \\ & (inout * read * d_p)(area_1 * inout * read * d_p) \ldots \\ & (area5 * inout * read * d_p)]. \end{aligned} \quad (18)$$

The values for each row of the random-effects design matrix Z are given by equation (19), where p is the participant where p_i is 1 for participant i and 0 otherwise. The mixed model was calculated using the restricted maximum likelihood method:

$$z(p, area, inout) = [p_1 \ldots p_{17}\ area_1\ area_2\ area_3\ area_4\ area_5\ inout]. \quad (19)$$

Each left and right TPA and frequency subband was analyzed with a separate mixed model. For each analysis, all effects, along with their interactions, were examined for significance and the model was simplified by removing the highest order nonsignificant interaction, or effect if no interaction existed, and recomputing the model. This simplification procedure was repeated until all effects and interactions in the model were significant with the exception that nonsignificant effects remained in the model if they were dependent effects of a significant interaction. This procedure has been widely used by ourselves and others (Frye et al. 2007; Frye, Fishcher, et al. 2008; Frye, Hasan, et al. 2008; Frye, Landry, et al. 2009). In order to verify that the statistical model represented the data accurately, diagnostic plots of standardized residual plots were examined to insure that the residuals demonstrated a normal distribution and that the predicted versus residual plots did not demonstrate any systematic bias. In order to mitigate the effects of inflated alpha due to performing multiple statistical models, we corrected the alpha for the full model using the Bonferroni method. Since there are 6 frequency bands examined and 2 TPAs (i.e., left and right) we used an alpha of 0.05/12 = ~0.004 for the overall analysis. All follow-up statistical tests used an alpha of 0.05. The relationship between performance and connectivity was additionally analyzed using 2-tailed Pearson correlations.

Results

Beta Frequency

Table 2 provides the *F* values for the mixed-model analyses for the beta frequency subbands.

Low Beta (12–14 Hz)

Left TPA. Connectivity was significantly influenced by an interaction between direction and performance, indicating that the relative balance between inward versus outward connectivity was related to task performance. As seen in Figure 2*A*, performance was related to the difference between inward and outward connectivity (r_{15} = –0.66, $P < 0.005$) such that better performance was associated with relatively greater outward connectivity from the left TPA to the other brain areas and a lower inward connectivity from the other regions of the brain to the left TPA.

Right TPA. Connectivity was influenced by an interaction among performance, direction, and reading group, indicating that the relative balance between inward versus outward connectivity was related to task performance but this was different across reading groups. Figure 2*B* demonstrates the relationship between performance and inward versus outward connectivity differences for both TRs and DRs. This relationship is significant for DRs (r_5 = 0.96, $P < 0.001$) but not TRs (r_8 = 0.40, $P > 0.10$). For DRs, greater relative inward connectivity from the rest of the brain areas to the right TPA was associated with relatively better performance, while greater relative outward connectivity from the right TPA to the rest of the brain areas was associated with relatively worse performance.

Middle Beta (15–19 Hz)

Left TPA. Connectivity significantly differed across cortical areas. Connectivity with the right TPA was significantly greater (t_{64} = 3.85, $P < 0.001$) than connectivity with other brain areas (Fig. 2*C*).

Right TPA. Connectivity significantly differed across cortical areas. Connectivity with the left TPA (t_{64} = 3.34, P = 0.001) and right IFA (t_{64} = 3.76, $P < 0.001$) was significantly greater than connectivity with other brain areas. In contrast (Fig. 2*D*), connectivity with the left IFA (t_{64} = 3.64, $P < 0.001$) was significantly lower than connectivity with other brain areas.

High Beta (20–29 Hz)

Left and right TPA connectivity did not differ across cortical area or reading groups and was not related to performance.

Gamma Frequency

Table 3 provides the *F* values for the mixed-model analyses and the *t* values for the planned contrasts for the gamma frequency.

Table 2

F values for the mixed-model analysis of the beta frequency subbands

	To	d′	In versus out	Reading	Reading × d′	In versus out × reading	In versus out × d′	Reading × d′ × in versus out
Low beta								
Left	5.4†	NS	NS				11.48†	
Right	5.0†	NS	NS	NS	NS	7.5¥	9.2¥	13.40†
Middle beta								
Left	6.15†							
Right	5.39†							

Note: NS, not significant.

*≤0.05, ¥≤0.01, †≤0.001, ‡≤0.0001.

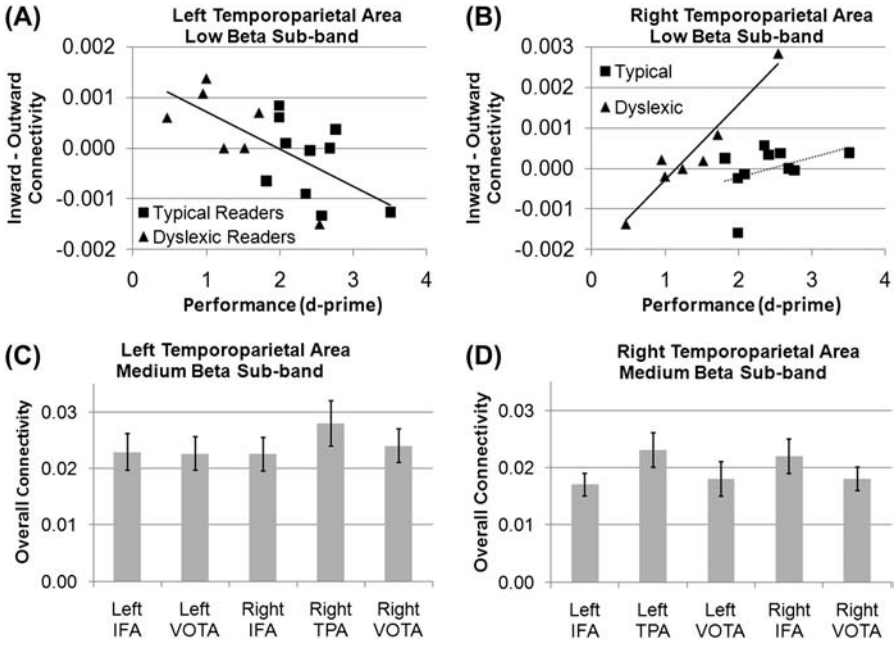

Figure 2. GC connectivity for the left and right TPAs for the low beta (*A*,*B*) and medium beta subbands (*C*,*D*). (*A*) The relationship between performance on the nonword phonological decoding task and the difference between inward and outward GC connectivity for the left TPA in the low beta subband. This relationship was significant across both TRs and DRs. Greater outward connectivity (as compared with inward connectivity) from the left TPA to other areas was associated with better nonword rhyme discrimination performance (d-prime). (*B*) The relationship between performance on the nonword phonological decoding task and the difference between inward and outward GC connectivity for the right TPA in the low beta subband. This relationship was only significant for DRs. Greater inward connectivity (as compared with outward connectivity) to the TPA from other brain areas was associated with better nonword rhyme discrimination performance (d-prime) in DRs. (*C*) Connectivity between the left TPA and the right TPA was greater than connectivity between the left TPA and the other cortical areas in the medium beta subband. (*D*) Connectivity between the right TPA and the left TPA and right IFA was greater than connectivity between the right TPA and other cortical areas in the medium beta subband. Error bars represent standard error.

Low Gamma (30–59 Hz)

Left TPA. Connectivity between the left TPA and other brain areas differed across brain area (Fig. 3*A*). This was due to the connectivity between the left TPA and the right TPA being greater than connectivity between the left TPA and other brain areas and connectivity between the left TPA and the left and right IFAs and VOTAs being lower than connectivity between the left TPA and other brain areas.

Right TPA. Connectivity between the right TPA and other brain areas significantly differed across brain area. This was due to the connectivity between the right TPA and both the left TPA and the right IFA being greater than connectivity between the right TPA and other brain areas and connectivity between the right TPA and the left IFA and VOTA and right VOTA being lower than connectivity between the right TPA and other brain areas (Fig. 3*B*).

Medium Gamma (60–89 Hz)

Left TPA. Connectivity between the left TPA and other brain areas differed across brain area. This was due to the relationship between the left TPA and the right TPA being greater than connectivity between the left TPA and other brain areas and connectivity between the left TPA and the left and right IFAs and VOTAs being lower than connectivity between the left TPA and other brain areas (Fig. 3*C*).

Right TPA. Connectivity between the right TPA and other brain areas differed across brain area. This was due to the connectivity between the right TPA and the left TPA and the right IFA being greater than connectivity between the right TPA and other brain areas and connectivity between the right TPA and the left IFA and VOTA and the right VOTA being lower than connectivity between the right TPA and other brain areas (Fig. 3*D*).

Table 3
F values for the mixed-model analysis of the beta frequency subbands and the *t* values for the planned contrasts

	Analysis of variance		Cortical area effect contrast					
	To	Reading	LF	LTP	LO	RF	RTP	RO
Low gamma								
Left	14.23‡	NS	−6.85‡		−6.74‡	−6.85‡	7.34‡	−7.05‡
Right	16.88‡	NS	−6.53‡	7.31‡	−6.36‡	6.51‡		−7.65‡
Middle gamma								
Left	14.54‡	NS	−7.00‡		−7.24‡	−6.59‡	8.63‡	−6.20‡
Right	16.51‡	NS	−5.95‡	6.91‡	−7.16‡	6.96‡		−7.40‡
High gamma								
Left	14.54‡	35.54‡	−7.66‡		−7.62‡	−7.80‡	8.08‡	−7.77‡
Right	13.26‡	NS	−6.78‡	7.12‡	−6.60‡	6.76‡		−6.87‡

Note: NS, not significant; LF, Left Frontal; LTP, Left Temporoparietal; LO, Left Occipital; RF, Right Frontal; RTP, Right Temporoparietal; RO, Right Occipital.
*≤0.05, ¥≤0.01, †≤0.001, ‡≤0.0001.

High Gamma (90–120 Hz)

Left TPA. Connectivity between the left TPA and other brain areas differed across brain area. This was due to the connectivity between the left TPA and the right TPA being greater than connectivity between the left TPA and other brain areas and connectivity between the left TPA and the left and the right IFAs and VOTAs being lower than connectivity between the left TPA and other brain areas (Fig. 3*E*).

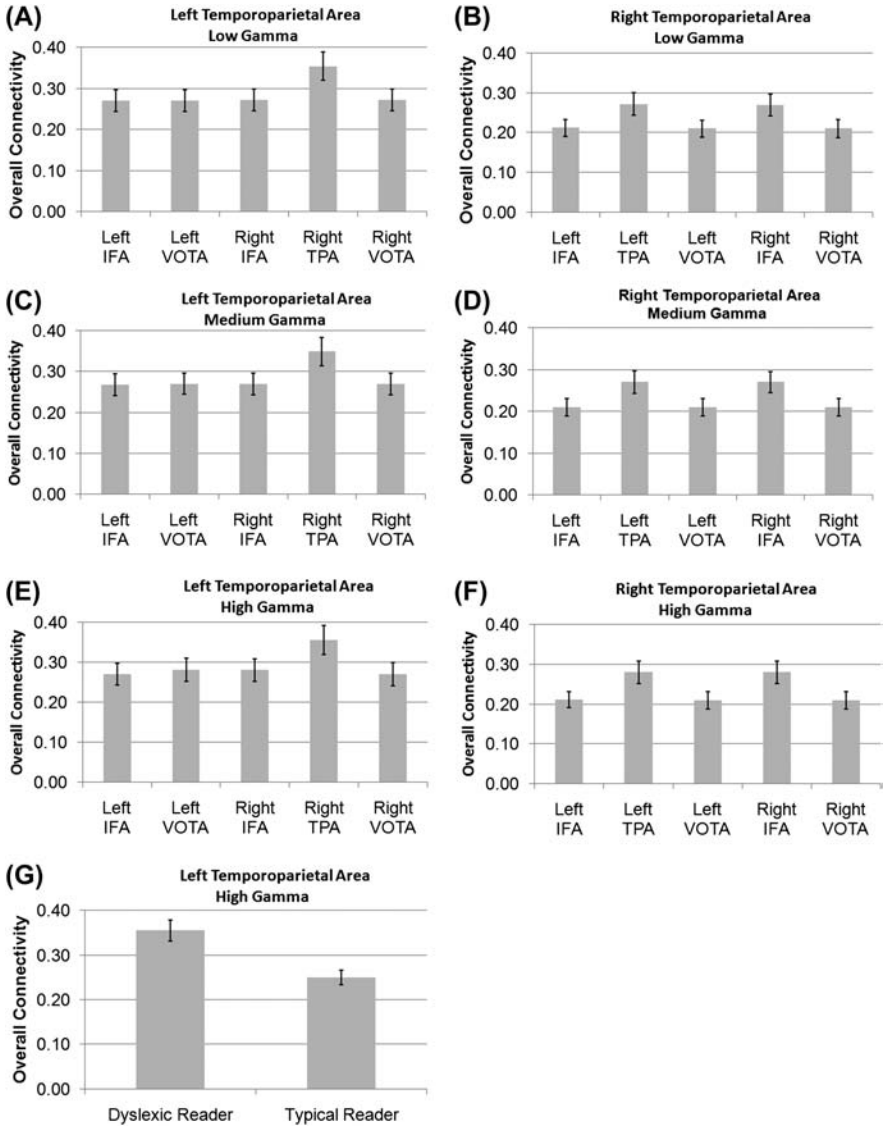

Figure 3. GC connectivity for the left (*A*,*C*,*E*,*G*) and right (*B*,*D*,*F*) TPAs for the low (*A*,*B*), medium (*C*,*D*), and high (*E*,*F*,*G*) gamma subbands. In general, the left TPA demonstrated greater connectivity with the right TPA as compared with other brain areas regardless of the subband (*A*,*C*,*F*) and the right TPA demonstrated greater connectivity with the left TPA and the right IFA regardless of the subband (*B*,*D*,*F*). (*G*) DRs demonstrated greater connectivity between the left TPA and other brain areas in the high gamma frequency subband as compared with TRs. Error bars represent standard error.

In addition, DRs were found to have significantly greater connectivity between the left TPA and all other brain areas as compared with TRs (Fig. 3*G*).

Right TPA. Connectivity between the right TPA and other brain areas differed across brain area. This was due to the connectivity between the right TPA and the left TPA and right IFA being greater than connectivity between the left TPA and other brain areas and connectivity between the right TPA and the left IFA and VOTA and right VOTA being lower than connectivity between the right TPA and other brain areas (Fig. 3*F*).

Discussion

This is the first study to compare effective neuromagnetic connectivity between the left and the right TPAs and other key areas of the brain necessary for phonological word decoding in DRs and TRs. This is also one of the first studies to examine effective connectivity during the prestimulus period. In this study, causal connectivity was analyzed in low, medium, and high beta and low, medium, and high gamma frequency subbands.

Across both reading groups the balance of inward versus outward connectivity to/from the left TPA to other regions of the brain was associated with phonological decoding performance. Note that there was no absolute difference between connectivity from the left TPA to other brain areas between DR and TR reading groups. This suggests that those that read best may use the TPA differently within the neural network responsible for preparing the brain for phonologically processing nonword stimuli than those that read poorly.

Our hypothesis with respect to the left TPA was confirmed within the low beta subband. In *For the Low Beta Frequency*

Subband, the Balance between Inward and Outward Connectivity to/from the Left TPA Was Related to Performance across Both Reading Groups, we will examine the implications of this finding. In contrast to our predictions for the left TPA, we hypothesized that greater right TPA control of other brain areas would be associated with poorer nonword decoding performance for DRs. This hypothesis was confirmed and the implication of this hypothesis will be discussed in *Greater Relative Outward Connectivity from the Right TPA to Other Brain Regions Was Associated with Relatively Worse Performance in DRs.* In *DRs Manifest Greater High Gamma Subband Effective Connectivity between the Left TPA and Other Regions,* we will discuss our finding that greater effective connectivity in the high gamma subband was associated with dyslexia. In *Future Studies to Examine the Generalizability of These Findings,* we will discuss the generalizability of our findings.

For the Low Beta Frequency Subband, the Balance between Inward and Outward Connectivity to/from the Left TPA Was Related to Performance across Both Reading Groups

Within all of the frequency bands, there were no overall group differences in inward versus outward connectivity to and from the TPA. In addition, the pattern of connectivity between the left versus the right TPA and other cortical regions was stable across frequency bands and reading groups.

However, there were definite differences in the relationship between task performance and the effective connectivity between the left TPA and other brain areas. For the low beta frequency subband, deviations from balanced inward as compared with outward connectivity had consequences for performance (Fig. 2). Those with greater connectivity from the left TPA to other cortical regions were more likely to have better phonological decoding and those with relatively greater connectivity into the left TPA from other regions were more likely to have worse phonological decoding performance, consistent with our hypothesis.

It is important to remember that the majority of participants irrespective of reading group had a relatively balanced inward as compared with outward connectivity between the left TPA and the other reading regions. Those with this balanced connectivity had d-prime scores over 1.0, indicating adequate discriminability of rhymes and nonrhymes. This suggests that for most of the participants, the left TPA was acting as more of an integration area rather than a control area. Specifically, participants with a balance between inward and outward connectivity may be using nonhierarchical small-world network topography.

In contrast, those participants who have greater outward as compared with inward left TPA connectivity may be using hierarchical network topography. Neural networks with hierarchical network topography have been shown to be more stable as compared with neural networks with nonhierarchical topography (Kaiser and Hilgetag 2010). This would be consistent with the findings of this study as the participants with greater outward left TPA connectivity, who therefore manifest a hierarchical TPA neural network topography, demonstrated better performance on the phonological nonword decoding task. Thus, having hierarchical network topography during the prestimulus period in the low beta frequency subband may stabilize the network so that it can optimally process the incoming nonword stimuli.

Greater Relative Outward Connectivity from the Right TPA to Other Brain Regions Was Associated with Relatively Worse Performance in DRs

We hypothesized that, as the degree of connectivity from the right TPA to the other nodes of the reading network increased, performance would decrease for DRs. This hypothesis was confirmed. This finding suggests that when the right TPA manifests increased influence over the other regions of the brain, performance was compromised. Combined with the findings discussed in *For the Low Beta Frequency Subband, the Balance between Inward and Outward Connectivity to/from the Left TPA Was Related to Performance across Both Reading Groups,* it appears that increased influence of the right TPA on the remainder of the brain is associated with a disruption in ascendancy of the left TPA in the network hierarchy, at least in DRs, resulting in a phonological decoding deficit. Specifically, the worst-performing DR had greater inward than outward functional connectivity between the left TPA and other brain areas and greater outward than inward functional connectivity between the right TPA and other brain areas. This suggests that DRs who have not attained an adequate ability to read may be doing so because the right TPA, rather than the left TPA, is acting as the control node in the phonological word decoding network. Since hierarchical network topography provides stability to the network structure, having a network with the right TPA as the control node may stabilize the neural network into a dysfunctional state.

The majority of functional imaging studies on DRs have reported greater right hemisphere TPA activation in DRs as compared with TRs (Simos, Breier, Fletcher, Bergman, et al. 2000; Simos, Breier, Fletcher, Foorman, et al. 2000; Temple, 2002; Heim and Keil 2004). Our results suggest that it is not merely the degree of activation which is important, but the direction of the functional connectivity of the right TPA with other brain areas involved in reading. Poorer phonological decoding in DRs was associated with increases in the influence of the right TPA upon the left TPA (as well as other brain areas). Studies using MEG have demonstrated that the timing to left and right TPA activation are reversed in DRs as compared with TRs. For example, TRs have been found to activate the left TPA approximately 118 ms prior to the right TPA, while DRs activate the right TPA approximately 123 ms before the left TPA during phonological decoding tasks (Simos, Breier, Fletcher, Bergman, et al. 2000). This pattern has also been reported in at-risk children (Simos, Breier, et al. 2002). These finding are consistent with the notion that (in some) DRs, increases in the influence of the right TPA on the left TPA may be related to quicker activation of the right TPA. Only some DRs in our sample had phonological task performance that was below chance and these were the DRs in which the right TPA appeared to be the control node of the network. Thus, we do not predict that all DRs have abnormal network topography. In fact, some MEG studies have not found these differences in timing between reading groups (Simos et al. 2005). This may be due to the fact that dipole waveforms comprise a wide frequency range, not just the beta frequency or its subbands, and measures such as waveform onset and/or peak latency derived from dipole source activations are not designed to measure the temporal relationship between sources. In contrast, GC and other casual connectivity techniques are specifically designed to examine the significance of the

relative changes in activity of sources. Alternatively, the lack of sensitivity to differences in network topography within reading groups may also be related to the DR sample studied.

Those DRs with an inadequate phonological rhyme task performance manifested excessive influence from the right TPA onto the remaining network. It is possible that the intrusion of excess right TPA influence prevents the establishment of a reading circuit with a dominant left TPA. Development of such an atypical language network could extend the period during which neuroplastic changes need to occur (from years to decades) before automatic and fluent reading skills can be established.

One question which arises is whether reading remediation training plays a role in reorganizing the prestimulus network and reestablishing a hierarchy. Focal and repeated use of a neural system followed by immediate feedback may enable the connections between neurons that facilitate phonological decoding to be strengthened and the connections that disrupt phonological processing to be weakened. This may be especially important in the case of dyslexia, in which migrational anomalies during gestation may disrupt normal patterns of connectivity. Training may serve to depress the contribution of these misplaced neurons. We suggest that one part of the decoding network which may need to be restructured is the outward connectivity of the right TPA to other cortical regions. In addition, our prior finding that greater influence of the left IFA outward to the TPA and VOTA (Frye, Wu, et al. 2010) is associated with better reading in DRs may indicate that the left IFA is working to encourage network reorganization in the brains of DRs.

Essentially the Same Patterns of Effective Connectivity Are Found between the Left TPA and Other Regions within the Medium and High Beta Subbands

Within the medium and high beta subband, there are 3 clear-cut patterns: 1) there is no significant inward or outward connectivity bias, 2) there is no performance or reading group factors related to connectivity, and 3) connectivity is stronger between the 2 TPAs than between any other region and either right or left TPAs. This suggested that the TPAs work together regardless of reading skill and/or whether the individual had a history of dyslexia as a child. Our previous study that examined IFA connectivity in DRs and TRs found similar findings. This suggests that the relationship within DRs between causal connectivity and their phonological decoding may be restricted to the low beta subbands and may not involve the medium and high beta subbands. However, with our limited sample size, changes within these subbands may be too subtle to detect.

Left TPA Underactivity Observed in DRs May Be Secondary to Diminished Left TPA Reactivity Rather Than Inadequate Input

Given that the connectivity between the left or the right TPAs and other brain areas key for phonological processes was not different between DRs and TRs for any frequency band, it is reasonable to presume that the left TPA, in particular, has an adequate inward connectivity, permitting it to be optimally stimulated. Since the left TPA is almost ubiquitously underactivated in DRs across functional neuroimaging studies (Pugh, Mencl, Jenner, et al. 2000), it is possible that the left TPA underarousal is due to reduced reactivity to input rather than lack of adequate input. This is consistent with our previous finding that top-down left IFA influence on other brain regions during the prestimulus period is positively correlated with performance in DRs (Frye, Wu, et al. 2010). In other words, the left IFA may be compensating for the reduced reactivity of the left TPA that normally occurs in TRs.

DRs Manifest Greater High Gamma Subband Effective Connectivity between the Left TPA and Other Regions

This study found greater high gamma subband effective connectivity between the left TPA and other regions in DRs but not TRs. This is consistent with our previous study which demonstrated that greater high gamma-band connectivity between the left IFA and other brain regions (i.e., right and left TPA and VOTA and right IFA) was associated with poorer performance on the phonological rhyme task, except that the effect found in the current study was specific to DRs. As discussed in the *Introduction,* during the prestimulus period, a relatively increased degree of gamma subband effective connectivity between the left TPA and other brain regions may be detrimental as intracranial EEG studies have demonstrated a transient desynchronization of gamma activity during reading in TRs (Lachaux et al. 2008). Since gamma-band synchronization has been proposed to facilitate communication between neighboring neurons to promote the formation of transient neural networks (Fries 2007), this finding may suggest that connections between local networks in and around the left TPA and other regions of the brain are not being decoupled in preparation for the processing of incoming stimuli. This could explain why the left TPA may have decreased reactivity to incoming stimuli. Specifically, if the neural networks in the left TPA do not transiently desynchronize, the neural networks in the left TPA may not be able to process new incoming stimuli adequately.

The fact that this finding is related to having dyslexia and is not associated with performance suggests that this could be one of the key reasons that the left TPA does not develop adequately during development. For example, if the left TPA does not readily desynchronize to allow new information to be integrated, especially during the acquisition of language, other areas of the brain, such as the homogenous regions in the right hemisphere (i.e., the right TPA) may take over the function of the left TPA. Such a shift in the laterality of language processing could start a detrimental cascade of events that leads to the right TPA becoming the control hub of the phonological decoding network. This notion is consistent with our finding that greater outward connectivity from the right TPA to other reading regions in the low beta subband is associated with poorer phonological decoding.

Future Studies to Examine the Generalizability of These Findings

This and our other recent study (Frye, Wu, et al. 2010) suggest that the hierarchical structure of the neural network that connect key brain areas important for reading differs for TRs and DRs with some of these differences being detrimental and others compensatory (specifically within the low beta subband during the preparatory period). This study did not examine any other stimuli besides nonwords, so it is not clear whether these changes are specific to words or phonological stimuli or represent general differences between the brains of

TRs and DRs. Future studies will need to investigate the differences in causal network structure in TRs and DRs across various stimuli.

Another major finding of this study and our previous study (Frye, Wu, et al. 2010) is that greater high gamma subband connectivity appeared to be detrimental. In our previous study where we examined the IFA, this finding was not specific to DRs but was related to performance for all participants. The current study found that higher left TPA gamma subband connectivity was specific to DRs. We interpreted this as an inability of the local neural networks to desynchronize and process new incoming information. It would be very important to determine when increased gamma connectivity was a general characteristic of DRs as it could explain more general problems in learning and processing speed that have been associated with DRs. Future studies should examine the ability of neural networks to shift and reorganize in DRs and TRs to determine if there is a role for such differences in dyslexia.

Conclusion

This study has demonstrated that prestimulus preparatory networks are reorganized in DRs and that network topography is directly associated with nonword rhyme performance. Reorganization of the prestimulus network associated with DRs was found in the low beta frequency subband. Although preliminary, our finding suggest that the left TPA is the important cortical hub for controlling and coordinating the preparatory neural network that subserves phonological nonword decoding and that this hub may be shifted toward the right hemisphere in DRs who have poor phonological decoding skills. In addition, we have found that increased interregional high gamma connectivity between the left IFA and other areas of the brain during the prestimulus period in DRs. This implicates a failure to decouple neural networks in the development of dyslexia. Further research will be needed to verify and expand on our findings. This combination of results demonstrates the importance of considering direction in connectivity analysis and suggests that analyses based on GC can help uncover the typical and atypical architecture of neural networks that underlie cognition.

Funding

This study was supported by grant NS046565 to R.E.F. and in part by Center of Excellence for Learning in Education, Science and Technology an National Science Foundation Science of Learning Center (SBE-0354378), J.L., Investigator.

Notes

Conflict of Interest : None declared.

References

Bitan T, Cheon J, Lu D, Burman DD, Booth JR. 2009. Developmental increase in top-down and bottom-up processing in a phonological task: an effective connectivity, FMRI study. J Cogn Neurosci. 21:1135–1145.

Brambati SM, Termine C, Ruffino M, Danna M, Lanzi G, Stella G, Cappa SF, Perani D. 2006. Neuropsychological deficits and neural dysfunction in familial dyslexia. Brain Res. 1113:174–185.

Cao F, Bitan T, Booth JR. 2008. Effective brain connectivity in children with reading difficulties during phonological processing. Brain Lang. 107:91–101.

Cohen D, Schalpfer U, Ahlfors S, Hamalainen M, Halgren E. 2002. New six-layer magnetically shielded room for MEG. Biomag Proceed.

Cornelissen PL, Kringelbach ML, Ellis AW, Whitney C, Holliday IE, Hansen PC. 2009. Activation of the left inferior frontal gyrus in the first 200 ms of reading: evidence from magnetoencephalography (MEG). PLoS One. 4:e5359.

Dale AM, Fischl B, Sereno MI. 1999. Cortical surface-based analysis. I. Segmentation and surface reconstruction. Neuroimage. 9:179–194.

Ding M, Bressler SL, Yang W, Liang H. 2000. Short-window spectral analysis of cortical event-related potentials by adaptive multivariate autoregressive modeling: data preprocessing, model validation, and variability assessment. Biol Cybern. 83:35–45.

Ding M, Chen Y, Bressler SL. 2006. Granger causality: basic theory and application to neuroscience. In: Schelter B, Winterhalder M, Timmer J, editors. Handbook of time series analysis. Berlin (Germany): Wiley-VCH. p. 451–474.

Dragovic M. 2004. Categorization and validation of handedness using latent class analysis. Acta Neuropsychiatr. 16:212–218.

Duncan-Milne R, Hamm JP, Kirk IJ, Corballis MC. 2003. Anterior-posterior beta asymmetries in dyslexia during lexical decisions. Brain Lang. 84:309–317.

Fischl B, Sereno MI, Dale A. 1999. Cortical surface-based analysis. II: inflation, flattening, and a surface-based coordinate system. Neuroimage. 9:195–207.

Florin E, Gross J, Pfeifer J, Fink GR, Timmermann L. 2009. The effect of filtering on Granger causality based multivariate causality measures. Neuroimage. 50:577–588.

Fries P. 2007. A mechanism for cognitive dynamics: Neuronal communication through neuronal coherence. Trends Cogn Sci. 9:474–480.

Fries P, Frye RE, Fisher JM, Coty A, Zarella M, Liederman J, Halgren E. 2007. Linear coding of voice onset time. J Cogn Neurosci. 19:1476–1487.

Frye RE, Fisher JM, Witzel T, Ahlfors SP, Swank P, Liederman J, Halgren E. 2008. Objective phonological and subjective perceptual characteristics of syllables modulate spatiotemporal patterns of superior temporal gyrus activity. Neuroimage. 40:1888–1901.

Frye RE, Hasan K, Xue L, Strickland D, Malmberg B, Liederman J, Papanicolaou A. 2008. Splenium microstructure is related to two dimensions of reading skill. Neuroreport. 19:1627–1631.

Frye RE, Landry SH, Swank PR, Smith KE. 2009. Executive dysfunction in poor readers born prematurely at high risk. Dev Neuropsychol. 34:254–271.

Frye RE, Liederman J, Hasan KM, Lincoln A, Malmberg B, McLean J, 3rd, Papanicolaou A. 2011. Diffusion tensor quantification of the relations between microstructural and macrostructural indices of white matter and reading. Hum Brain Mapp. 32:1220–1235.

Frye RE, Liederman J, Malmberg B, McLean J, Strickland D, Beauchamp MS. 2010. Surface area accounts for the relation of gray matter volume to reading-related skills and history of dyslexia. Cereb Cortex. 20:2625–2635.

Frye RE, Wu MH. Forthcoming. Multichannel least-squares linear regression provides a fast, accurate, unbiased and robust estimation of Granger causality for neurophysiological data. Comput Biol Med.

Frye RE, Wu MH, Liederman J, Fisher JM. 2010. Greater pre-stimulus effective connectivity from the left inferior frontal area to other areas is associated with better phonological decoding in dyslexic readers. Front Syst Neurosci. 4:156.

Geweke JF. 1984. Measures of conditional linear dependence and feedback between time series. J Am Stat Assoc. 79:907–915.

Granger CWJ. 1969. Investigating causal relations by econometric models and cross-spectral methods. Econometrica. 37:424–438.

Gross J, Schmitz F, Schnitzler I, Kessler K, Shapiro K, Hommel B, Schnitzler A. 2004. Modulation of long-range neural synchrony reflects temporal limitations of visual attention in humans. Proc Natl Acad Sci U S A. 101:13050–13055.

Gross J, Schmitz F, Schnitzler I, Kessler K, Shapiro K, Hommel B, Schnitzler A. 2006. Anticipatory control of long-range phase synchronization. Eur J Neurosci. 24:2057–2060.

Hämäläinen M, Hari R, Ilmoniemi R, Knuutila J, Lounasmaa O. 1993. Magnetoencephalography—theory, instrumentation, and applications to noninvasive studies of the working human brain. Rev Mod Phys. 65:1–93.

Heim S, Keil A. 2004. Large-scale neural correlates of developmental dyslexia. Eur Child Adoles Psychiatry. 13:125–140.
Horwitz B, Rumsey JM, Donohue BC. 1998. Functional connectivity of the angular gyrus in normal reading and dyslexia. Proc Natl Acad Sci U S A. 95:8939–8944.
Hosoya Y. 2001. Elimination of third-series effect and defining partial measures of causality. J Time Ser Anal. 22:537–554.
Kaiser M, Hilgetag CC. 2010. Optimal hierarchical modular topologies for producing limited sustained activation of neural networks. Front Neuroinform. 4:8.
Kaminski MJ, Blinowska KJ. 1991. A new method of the description of the information flow in the brain structures. Biol Cybern. 65:203–210.
Lachaux JP, Jung J, Mainy N, Dreher JC, Bertrand O, Baciu M, Minotti L, Hoffmann D, Kahane P. 2008. Silence is golden: transient neural deactivation in the prefrontal cortex during attentive reading. Cereb Cortex. 18:443–450.
Levy J, Pernet C, Treserras S, Boulanouar K, Aubry F, Demonet JF, Celsis P. 2009. Testing for the dual-route cascade reading model in the brain: an fMRI effective connectivity account of an efficient reading style. PLoS One. 4:e6675.
Mainy N, Jung J, Baciu M, Kahane P, Schoendorff B, Minotti L, Hoffmann D, Bertrand O, Lachaux JP. 2008. Cortical dynamics of word recognition. Hum Brain Mapp. 29:1215–1230.
Matsumoto A, Iidaka T. 2008. Gamma band synchronization and the formation of representations in visual word processing: evidence from repetition and homophone priming. J Cogn Neurosci. 20:2088–2096.
McGraw Fisher J, Liederman J, Johnson J, Lincoln A, Frye RE. Forthcoming. A demonstration that task difficulty can confound the interpretation of lateral differences in brain activation between typical and dyslexic readers. Laterality.
Miller-Shaul S. 2005. The characteristics of young and adult dyslexics readers on reading and reading related cognitive tasks as compared to normal readers. Dyslexia (Chichester, England). 11:132–151.
Pennington BF, Lefly DL. 2001. Early reading development in children at family risk for dyslexia. Child Dev. 72:816–833.
Penolazzi B, Spironelli C, Vio C, Angrilli A. 2010. Brain plasticity in developmental dyslexia after phonological treatment: a beta EEG band study. Behav Brain Res. 209:179–182.
Pugh KR, Mencl WE, Jenner AR, Katz L, Frost SJ, Lee JR, Shaywitz SE, Shaywitz BA. 2000. Functional neuroimaging studies of reading and reading disability (developmental dyslexia). Ment Retard Dev Disabil Res Rev. 6:207–213.
Pugh KR, Mencl WE, Shaywitz BA, Shaywitz SE, Fulbright RK, Constable RT, Skudlarski P, Marchione KE, Jenner AR, Fletcher JM, et al. 2000. The angular gyrus in developmental dyslexia: task-specific differences in functional connectivity within posterior cortex. Psychol Sci. 11:51–56.
Quaglino V, Bourdin B, Czternasty G, Vrignaud P, Fall S, Meyer ME, Berquin P, Devauchelle B, de Marco G. 2008. Differences in effective connectivity between dyslexic children and normal readers during a pseudoword reading task: an fMRI study. Neurophysiol Clin. 38:73–82.
Sakkalis V. Forthcoming. Review of advanced techniques for the estimation of brain connectivity measured with EEG/MEG. Comput Biol Med.
Sameshima K, Baccala LA. 1999. Using partial directed coherence to describe neuronal ensemble interactions. J Neurosci Methods. 94:93–103.
Seth AK, Edelman GM. 2007. Distinguishing causal interactions in neural populations. Neural Comput. 19:910–933.
Shaywitz BA, Lyon GR, Shaywitz SE. 2006. The role of functional magnetic resonance imaging in understanding reading and dyslexia. Dev Neuropsychol. 30:613–632.
Shaywitz SE. 1998. Current concepts: dyslexia. N Engl J Med. 338: 307–312.
Shaywitz SE, Shaywitz BA. 2008. Paying attention to reading: the neurobiology of reading and dyslexia. Dev Psychopathol. 20:1329–1349.
Shaywitz SE, Shaywitz BA, Fulbright RK, Skudlarski P, Mencl WE, Constable RT, Pugh KR, Holahan JM, Marchione KE, Fletcher JM, et al. 2003. Neural systems for compensation and persistence: young adult outcome of childhood reading disability. Biol Psychiatry. 54:25–33.
Simos PG, Breier JI, Fletcher JM, Bergman E, Papanicolaou AC. 2000. Cerebral mechanisms involved in word reading in dyslexic children: a magnetic source imaging approach. Cereb Cortex. 10:809–816.
Simos PG, Breier JI, Fletcher JM, Foorman BR, Bergman E, Fishbeck K, Papanicolaou AC. 2000. Brain activation profiles in dyslexic children during non-word reading: a magnetic source imaging study. Neurosci Lett. 290:61–65.
Simos PG, Breier JI, Fletcher JM, Foorman BR, Francis DJ, Castillo EM, Davis RN, Fitzgerald M, Mathes PG, Denton C, et al. 2002. Brain activation profiles during the early stages of reading acquisition. J Child Neurol. 17:159–163.
Simos PG, Fletcher JM, Bergman E, Breier JI, Foorman BR, Castillo EM, Davis RN, Fitzgerald M, Papanicolaou AC. 2002. Dyslexia-specific brain activation profile becomes normal following successful remedial training. Neurology. 58:1203–1213.
Simos PG, Fletcher JM, Foorman BR, Francis DJ, Castillo EM, Davis RN, Fitzgerald M, Mathes PG, Denton C, Papanicolaou AC. 2002. Brain activation profiles during the early stages of reading acquisition. J Child Neurol. 17:159–163.
Simos PG, Fletcher JM, Sarkari S, Billingsley RL, Denton C, Papanicolaou AC. 2007. Altering the brain circuits for reading through intervention: a magnetic source imaging study. Neuropsychology. 21:485–496.
Simos PG, Fletcher JM, Sarkari S, Billingsley RL, Francis DJ, Castillo EM, Pataraia E, Denton C, Papanicolaou AC. 2005. Early development of neurophysiological processes involved in normal reading and reading disability: a magnetic source imaging study. Neuropsychology. 19:787–798.
Snowling MJ. 2008. Specific disorders and broader phenotypes: the case of dyslexia. Q J Exp Psychol. 61:142–156.
Spironelli C, Penolazzi B, Angrilli A. 2008. Dysfunctional hemispheric asymmetry of theta and beta EEG activity during linguistic tasks in developmental dyslexia. Biol Psychol. 77:123–131.
Svensson I, Jacobson C. 2006. How persistent are phonological difficulties? A longitudinal study of reading retarded children. Dyslexia (Chichester, England). 12:3–20.
Temple E. 2002. Brain mechanisms in normal and dyslexic readers. Curr Opin Neurobiol. 12:178–183.
Temple E, Deutsch GK, Poldrack RA, Miller SL, Tallal P, Merzenich MM, Gabrieli JD. 2003. Neural deficits in children with dyslexia ameliorated by behavioral remediation: evidence from functional MRI. Proc Natl Acad Sci U S A. 100:2860–2865.
Trebuchon-Da Fonseca A, Benar CG, Bartolomei F, Regis J, Demonet JF, Chauvel P, Liegeois-Chauvel C. 2009. Electrophysiological study of the basal temporal language area: a convergence zone between language perception and production networks. Clin Neurophysiol. 120:539–550.
von Stein A, Rappelsberger P, Sarnthein J, Petsche H. 1999. Synchronization between temporal and parietal cortex during multimodal object processing in man. Cereb Cortex. 9:137–150.
Wechsler D. 1997. Wechsler adult intelligence scale-III (WAIS-III). New York: Psychological Corporation.
Wu MH, Frye RE, Zouridakis G. Forthcoming. A comparison of multivariate causality based measures of effective connectivity. Comput Biol Med.
Yap RL, van der Leij A. 1994. Testing the automatization deficit hypothesis of dyslexia via a dual-task paradigm. J Learn Disabil. 27:660–665.